



Research paper

Probabilistic analysis of the mesh load factor in wind-turbine planetary transmissions: Tooth thickness errors

A. Diez-Ibarbia^{a,*}, J. Sanchez-Espiga^a, A. Fernandez-del-Rincon^a, J. Calvo-Irisarri^b,
M. Iglesias^a, F. Viadero^a

^a Departamento de Ingeniería Estructural y Mecánica, Universidad de Cantabria Avda, Los Castros s/n, 39005, Santander, Spain

^b Siemens Gamesa Renewable Energy, Parque Tecnológico de Bizkaia, Zamudio, 48170, Spain

ARTICLE INFO

Keywords:

Mesh load factor K_f
Planetary transmission
Methods of Monte Carlo and Taguchi
Tooth thickness error

ABSTRACT

This manuscript presents a probabilistic analysis of the mesh load factor in planetary transmissions destined to the wind-turbine industry. This work main goal is to stochastically evaluate the impact of the planetary gears manufacturing processes uncertainties on the transmission performance, depending on their geometric configuration. In order to establish this analysis, the tooth thickness error effect on the transmission performance is chosen, and several tolerances considered in DIN-3967 are statistically analysed. In this regard, two statistical methods – Monte Carlo's Method and Taguchi's Method – are compared for equally spaced in phased and sequentially phased configurations. This comparison allows to assess the accuracy of both methods, taking into account the significant difference in the necessary number of cases, which reaches 20,000 for Monte Carlo's. Furthermore, a tolerance sensitivity analysis was performed to assess the influence of the errors size on the transmission performance, represented by its mesh load factor. Finally, the results show the number of non-valid transmissions compared to the threshold set by the IEC-61400.

1. Introduction

Gearboxes are one of the essential elements in plenty of applications because of their inherent characteristics, such as durability, compactness, robustness and high efficiency with respect to other possible solutions [1–6]. Their main goal is to transfer and adapt the energy provided by the power source, losing the lesser power during their performance. In some of these applications, this process of energy transference is conveyed by planetary gear transmissions, which allow to adapt the power sources operating conditions to several torque and speed requirements, being this versatility, among other characteristics, the reason why they are so widely used. Nevertheless, planetary gearboxes have more components than an ordinary gear transmission, in which only one gear ratio could be obtained. Thus, their behaviour is more complex and is potentially more affected by the inherent manufacturing errors of their components.

In this case application, wind-energy planetary gearboxes are to be studied, since they are key for the wind turbines performance [7–11]. This mechanical system is in charge of adequating the input wind power to the required speed and torque conditions of the electric generator. Wind energy is the most extended renewable energy nowadays. Hence, improving their performance will have a huge impact on the society evolution to a better and greener technology.

Regarding the gearboxes manufacturing process, as is well known, the degree of repeatability of a product characteristics is not the unity. This means that when a transmission is manufactured, even if the same conditions apply (temperature, humidity,

* Corresponding author.

E-mail address: alberto.diez@unican.es (A. Diez-Ibarbia).

same machine tool, material, etc.), the probability of obtaining the same result, in terms of its characteristics, it is not one hundred percent. This kind of process is usually denominated as stochastic, whilst it is called deterministic when the degree of repeatability is the unity.

In manufacturing processes, this is generally caused by two kinds of errors, one systematic and another random. The former is usually related to poor calibration or operation of the manufacturing machine/tool, temperature and environmental conditions, among other factors, and the latter, of random nature, it is associated with intangible phenomena of the process itself. All this leads to an undeniable uncertainty when it comes to predicting the results of the product characteristics. It is for all of the above that, even if the same input variables are included, the outputs of the process will behave as random variables, which will have probability functions associated with them. Therefore, one of the challenges of this work is to include these probabilistic variables in an a-priori deterministic numerical model.

One of the main objectives of this proposal is to include the uncertainty associated with the planetary gears manufacturing processes into the model previously developed by the authors [12–15]. More specifically, as major contribution, it is intended to evaluate the effect of the planet tooth thickness errors uncertainty on the working characteristics of the planetary transmission, under two kinds of configurations (equally spaced in phase and sequentially phased), taking into account the standard thresholds in the field of wind generators. The purpose of this work is to shed some light about the effect of the planetary gears manufacturing processes uncertainties on the transmission performance stochastically depending on their geometric configuration, since only deterministic model information can be found on the state of the art [13,14,16,17]. In this regard, the chosen parameter to be analysed is the mesh load factor, also called K_v factor, which measures how loaded the planets are with respect to their ideal load, and therefore, it is closely related to planetary transmissions malfunctioning [18]. This is the reason why there are specific planetary gear regulations, which require that this K_v value does not exceed a threshold. In wind energy gearboxes application, this threshold is generally regulated by IEC-61400 standard [19] and varies depending on the number of planets. Moreover, regarding the thickness error, DIN-3967 [20] sets the tolerance according to the gear geometry.

This work is the result of a research project developed with a manufacturer of wind-turbine planetary gear transmissions. The outcomes of this research show to what extent increasing the manufacturing quality of the tooth error results in a lower mesh load factor. This fact greatly affects the production and manufacturing costs (the higher the quality, the higher the manufacturing costs), however, if the mesh load factor is significantly lower, this turns into a longer transmission life, reducing maintenance costs. Therefore, the results can be directly applied to the design of wind-turbine planetary gear transmissions, as the trade-off between production costs and improved behaviour can be established. For this purpose, the assessment of a real gearbox manufacturing process was required. This wind-turbine planetary gear transmission manufacturer provided some real data of its manufacturing process that, because of confidentiality reasons, cannot be disclosed. Thus, in order to overcome this contingency, the information has been processed and subsequently adapted to a different planetary gear transmission for investigation publication purposes.

Furthermore, a study of applications, which use methodologies that include uncertainties of any kind in deterministic numerical models, has been carried out, with special emphasis on the design and analysis of gear transmissions. Regarding the statistical methods analysed, the so-called “Method of Monte Carlo” (MMC) is the most widespread and oldest of them. It can be defined as a series of mathematical/statistical methods utilised to obtain a probabilistic solution to a stochastic process. Whilst, Taguchi’s method is presented as an efficient tool for the design and optimisation of processes and products [21]. From a methodological point of view, this method is based on the concept of randomisation and analysis of variance to ensure robust, high quality and low cost products [22].

The MMC has been applied to several industrial sectors to incorporate the uncertainties of a real process. From logistics [23], to financial sector [24], including construction [25] and energy sectors [21,26–28]. Precisely, in the energy sector, these techniques have been extensively employed in renewable energy, since their power sources are of random nature, such as wind [22,29,30], sun [31] and water [32–34]. Of course, these methodologies have also been applied to mechanical design of elements and systems and, therefore, in gear transmissions [35–37].

The Taguchi’s method has been also extensively used and compared with the former in several applications, among which the design of gear transmissions stands out [38–45]. Sundaresan et al. [45] employed this method to analyse the effect of gear parameters (pressure angle, addendum and number of pinion teeth and tool addendum) derived from the uncertainty of the manufacturing process, on the maximum bending stress value of the tooth. Mayeux et al., in [42], employed Taguchi’s method to study the variability of misalignments and preload in bearing stiffness and gear stiffness, as well as the static transmission error. Rigaud, in [44], evaluated the variability of the spur gear transmission critical speed induced by misalignment and manufacturing errors in the teeth, using the two methods under study.

As synthesis of the state of knowledge in this regard, it can be established that MMC is, by far, the method that provides more information. Nevertheless, its main disadvantage is the high computational cost that it entails. Taguchi’s method does not provide as detailed information as MMC, but it considerably reduces the number of simulations to be carried out. Thus, a compromise between precision and computational effort is obtained by this method. In this study, in order to quantify the error between methods in this application and to select the more interesting to characterise the K_v , it has been deemed convenient to apply and compare both methodologies, in the assessment of the uncertainty associated with the planet thickness error inherent to its manufacturing processes, in equally spaced planetary gear transmissions in phase and sequentially phased.

After this introduction, Section 2 presents the fundamentals and methodologies required to develop and understand the analyses. Then, the main parameters of the planetary gear transmissions, as well as the test set-up, are described in Section 3. In Section 4, the results are discussed, to finish with some conclusions in Section 5. Moreover, it has been deemed interesting to include a parallel study performed during MMC analysis, regarding the number of cases to be performed. This study, which is shown in the appendix “Stop criteria”, was decisive to determine the number of MMC simulations and could be instructive to other stochastic analysis.

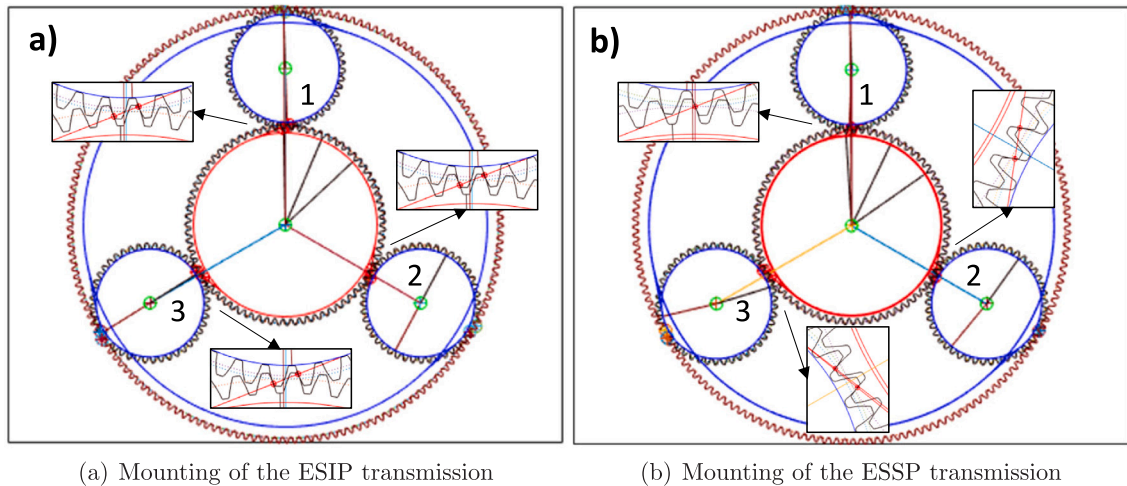


Fig. 1. Gears mounting of the ESIP (left) and ESSP (right) configurations.

2. Fundamentals and methodologies

In this section, a compilation of the fundamentals and methodologies required to develop and comprehend the analysis is presented. Firstly, some features of the numerical gear transmission model previously developed by the authors are detailed. Secondly, the different kinds of planetary gear transmission configurations, regarding the phase and spacing among planets, are shown, specifying the ones used in this study. Then, the tooth thickness error formulation implemented in the planetary gear transmission model is shown. Lastly, a summary of the statistical methodologies employed for including the uncertainty associated with manufacturing process of the gears is described.

2.1. Numerical model developed by the authors

In order to achieve the work final aim successfully, the pros and cons of the available approaches to develop the numerical model were assessed. On the one hand, lumped parameter and analytical models lead to a simpler approach to solving the behaviour of planetary transmissions. Nevertheless, these models, due to their definition and formulation, are normally applied to the resolution of the dynamic problem. On the other hand, finite element (FE) models provide the detailed definition of the behaviour. However, these exponentially increase computational times and FE analysis has inherent problems in contact resolution. A correct determination of the phenomena that occur in the contact region and its surroundings by finite element models requires an extreme refinement in the mesh, or an annexed algorithm in order to be able to analytically solve the contact problem (hybrid model). In addition, this refinement in the mesh would have to be considered for each study position throughout the simulation and, therefore, redefine the mesh for each iteration. Finally, the hybrid models, where analytical definitions are used in the contact or multi-body models for the kinematics of the transmission, seem to be the best option in search of a balance between sufficient precision in the results and acceptable computational time. Hybrid models with a quasi-static approach enable detailed analysis, using valid approximations to provide a simpler solution to the conflicting points of the modelling, with an affordable computational effort. In conclusion, with an objective such as the one proposed in this work, where more than 150,000 cases were to be performed, a hybrid model is considered the best option, seeking a balance between calculation accuracy and computational time.

The gear transmission model developed by the authors has been presented extensively in [12,46–48] and its development also for planetary transmissions in [13–15,49]. As an example, Fig. 1 shows the mounting of the two transmission configurations used in this work.

The main strength of the model resides in the contact forces calculation methodology, which consists of an enhanced procedure that involves the local and global deformations of the wheels, as well as the viscous and friction forces for internal and external gear meshes (Fig. 2). Since, in this case of study, there is a 3-planet planetary gear set involved (6+ contacts for a conventional contact ratio ($1 < \epsilon_\alpha < 2$)), the calculation accuracy of each contact will have a huge impact in the resulting behaviour and is key to obtain a reliable K_v value.

The resolution of these contacts and the balance in the transmission are fruit of iterative processes. Every contact employs an iterative procedure with a Weber–Banaschek formulation [50], adapted also for internal gears in [13], to solve the local contact problem, which is non-linear. These are added to the linear part of the contact, which is related to the deformations obtained in the FE models and solved following Vedmar's approach [51]. The FE models are planar and meshed composed by linear triangular elements, using the Partial Differential Equations Toolbox in MATLAB®. With respect to the boundary conditions, the shaft mounting is considered fully embedded. Then, the solutions to the contact between each pair of wheels are gathered together and formulated

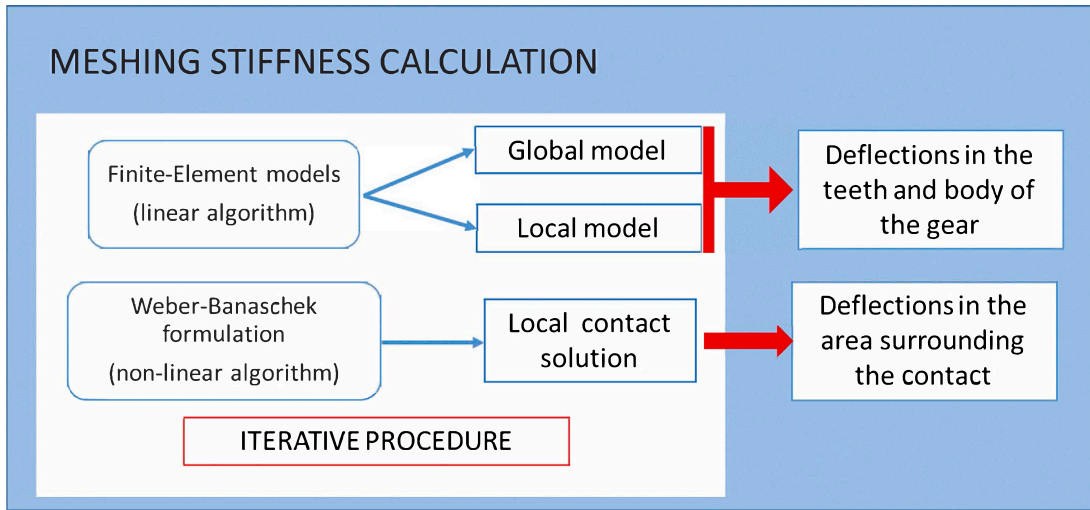


Fig. 2. Calculation of the meshing stiffness by using the FE models and Weber–Banaschek.

Table 1
Geometrical conditions for planetary transmissions.

Assembly configuration	Mathematical conditions		
Acronym	Spacing	Phase	Sequence
ESSP	$\psi_i = \frac{2\pi(i-1)}{N}$	$\frac{Z_r \psi_i}{2\pi} \neq n$	$\sum_{i=1}^N Z_r \psi_i = m\pi$
NESIP	$\psi_i \neq \frac{2\pi(i-1)}{N}$	$\frac{Z_r \psi_i}{2\pi} = n$	
NESSP	$\psi_i \neq \frac{2\pi(i-1)}{N}$	$\frac{Z_r \psi_i}{2\pi} \neq n$	$\sum_{i=1}^N Z_r \psi_i = m\pi$
NESAP	$\psi_i \neq \frac{2\pi(i-1)}{N}$	$\frac{Z_r \psi_i}{2\pi} \neq n$	$\sum_{i=1}^N Z_r \psi_i \neq m\pi$

in order to be able to establish the balance problem in the transmission. In the case of the current work, this balance is limited to the torque transmission in the sun (Eq. (1)) and the torque balance in each planet (Eq. (2)).

$$\vec{T}_{in} = \sum_{i=1}^N \vec{F}_{sp_i} \times \vec{r}_s \tag{1}$$

$$\vec{F}_{sp_i} \times \vec{r}_{p_i} = \vec{F}_{pr_i} \times \vec{r}_{p_i} \tag{2}$$

Where \vec{F}_{sp_i} & \vec{F}_{pr_i} are the contact forces in the sun-planet and planet-ring contacts for planet i , \vec{r}_s & \vec{r}_{p_i} are the base radii of the sun and the planet i , N is the number of planets, in this case study three, and \vec{T}_{in} corresponds to the planetary transmission input torque.

Once the iterations in the balance problem converge and the contact forces are accurately calculated, the Load Sharing Ratio (LSR_i) in the transmission can be consequently obtained following Eq. (3).

$$LSR_i = \frac{F_{sp_i}}{\sum_{j=1}^N F_{sp_j}} \tag{3}$$

Where the F_{sp_i} corresponds to the magnitude of contact force between sun and planet in planet i , and LSR_i is the load sharing ratio in planet i with respect to the total load in the transmission. The K_γ is directly related to the LSR as stated in Eq. (4).

$$K_\gamma = \max(N \cdot LSR_i) \tag{4}$$

2.2. Planetary transmissions configurations

Focusing on their geometry, planetary transmissions can be categorised in different ways, one of those classifications would establish five classes depending on their planet spacing and the mesh phasing amongst their contacts. They are summarised in Table 1 together with the analytical conditions to verify each of the categories.

Where ESIP stands for Equally Spaced In-Phase transmission, ESSP for Equally Spaced Sequentially Phased transmissions, NESIP for Non-Equally Spaced In-Phase transmission, NESSP for Non-Equally Spaced Sequentially Phased transmission, and NESAP for

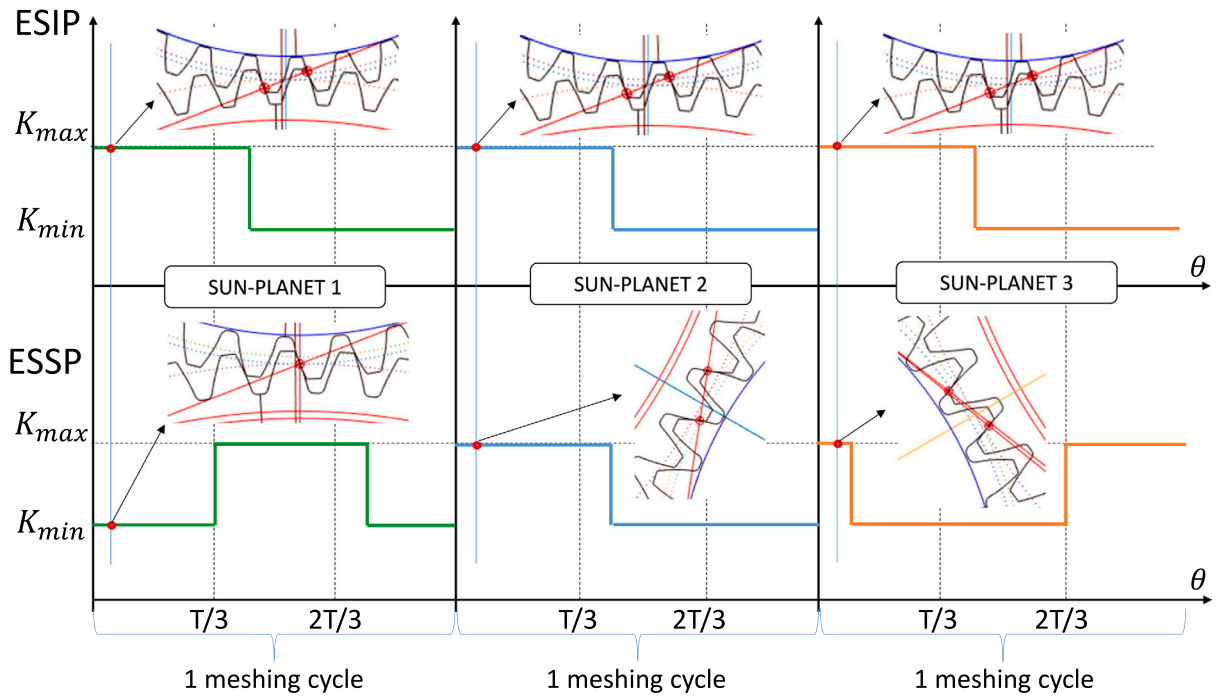


Fig. 3. Sun-Planet meshing stiffness comparison between ESIP and ESSP configurations of a 3-planet transmission.

Non-Equally Spaced Arbitrarily Phased transmission respectively, as gathered in [14]. Regarding the variables used for the analytical expressions, ψ_i refers to the i -planet angular spacing, N is the number of planets, Z_r is the number of teeth in the ring gear, and n & m are integers.

Equally spaced means that the angular distribution of the planets along the planet carrier surrounding the sun gear is uniform. Thus, the angular distance between consecutive planets is the same, and for this work this angle is $2\pi/3$ rad, being a direct consequence of the number of planets. Whenever this condition is not fulfilled, the planets are non-equally spaced.

On the other hand, the phase gives information about the contacts in the transmission. More precisely, the phase gives information about all the contact between sun and planets or between planets and ring gear. For an “In Phase” transmission every contact between sun and planets or planets and ring happen exactly at the same time. Thus, every contact is located at the same point along the meshing line, as the rest of the same kind in the same moment in time. On the contrary, the transmissions considered “Sequentially Phased” present a delay in the contacts between sun and planets or planets and ring. This delay can be uniform, for the transmissions where the planets are “Equally Spaced”, however, this delay will not be uniform in the ones where the planets are “Non-Equally Spaced”. This uniformity means that the contacts describe a sequence in which the delay is equal to the meshing cycle period divided by the number of planets, therefore, T/N , so $T/3$ in the configurations studied in the current work. For Non-Equally Spaced transmissions not only will this sequence not be uniform, but also will it fulfil the third requirement to be arbitrarily phased. Nonetheless, in the performance of these transmissions, it is not perfectly clear the difference between NESSP and NESAP, at least as far as its load sharing is concerned.

In this study, the scope of transmissions is limited to the ones where the planets are “Equally Spaced” (ESIP and ESSP). These correspond to the most common configurations used in industrial applications, and more precisely, in the wind generator industry. In order to illustrate what has been described above regarding the influence of the mesh phasing, in Fig. 3 the ideal meshing stiffness in each sun-planet contact and its detail are shown.

2.3. Tooth thickness error

As stated before in Section 2.1, the model employed for the simulations provides the opportunity to include an extensive variety of manufacturing and mounting errors in the planetary transmission. One of the more common manufacturing errors in planetary transmissions is the tooth thickness error, which has a great influence in the load sharing behaviour comparable to that of the tangential pin positioning error [13,14,16,17]. This error corresponds to the difference between the measured and the ideal value of the distance between opposed flanks in a number of teeth, denominated commonly as chordal distance. This distance is obtained following the procedure detailed by Wildhaber in [52], where the number of teeth considered varies with the size of the wheel. However, in order to model this error in a simpler manner, the approach taken differs to the mentioned procedure. Firstly, every single value of the measurements of chordal distance in all the planets (w_{k_i}) that belong to the same transmission are taken. Then,

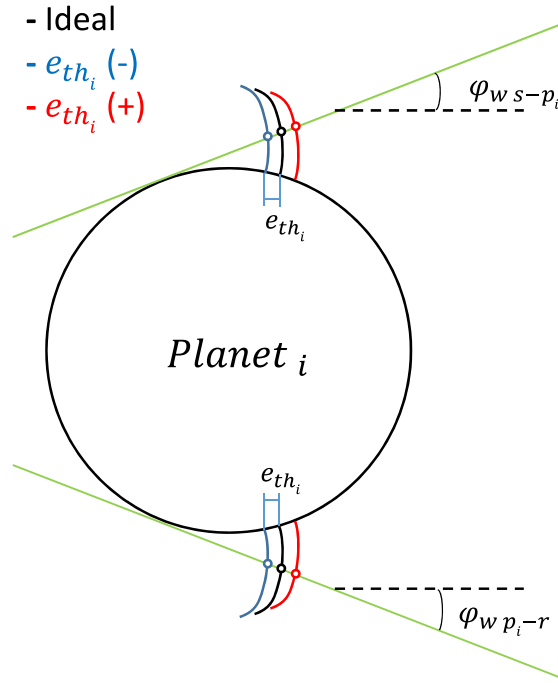


Fig. 4. Impact of the tooth thickness error in the geometry of the contacts.

the average value of every measurement is obtained (w_k^{avg}) and the difference between each measured and the average value of all the measurements is calculated (e_{th_i}), as shown in Eq. (5). Thus, every considered tooth thickness error is referred to the average of all the chordal distances and therefore every scenario is comparable.

$$e_{th_i} = w_{k_i} - w_k^{avg} \rightarrow w_k^{avg} = \frac{\sum_{i=1}^M w_{k_i}}{M} \tag{5}$$

Where subindex i correspond to the specimen number and M to the total number of measured specimens. Furthermore, as relevant statement, a transmission, in which all the planets have an equal and different-to-zero tooth thickness error, will not be affected on its load sharing, since every contact with every planet will be identical, only advanced or delayed with respect to the ideal mounting scenario.

Taking into consideration every aspect commented above, the mentioned e_{th_i} values are included in the geometrical algorithm employed for the calculation of the overlaps between active flanks. Thus, the overlap is directly modified by the e_{th_i} , which is added in the pressure angle direction to consider its effect, following Eq. (6).

$$\delta_{u,v} = \delta_{o_{u,v}} + e_{th_i} \cdot \cos(\varphi_{w_{u,v}}) \tag{6}$$

Where $\delta_{u,v}$ is the overlap between the active flanks of the wheels u and v (u and v may be sun, planet or ring), subindex o shows that overlap is the calculated originally without the effect of the tooth thickness error and $\varphi_{w_{u,v}}$ is the nominal pressure angle of the wheels.

The impact that this error has on the performance of the transmission is related to the contacts amongst sun-planet and planet-ring. This effect is illustrated in Fig. 4, where the inclusion of a change in the tooth thickness produces an advance or delay at the beginning of the contact between active flanks. Furthermore, it modifies the position of the contact along the meshing line. Therefore, it would be possible to also see a mesh phasing alteration due to the different tooth thickness, as shown previously by Sanchez-Espiga et al. in [14].

In this study, the same tooth thickness error has been implemented to all the planet teeth and flanks, having each planet of the transmission a different value incorporated randomly. Generally, this error has a limit tolerance regulated by standards, which varies depending on the application. In this case study (wind turbines), DIN-3967 [20] has been used as reference, where this tolerance value is obtained taking into account the dimensions and characteristics of the transmission gears. In Table 2, a fragment of this standard is compiled, which establishes that for a “cd24” gear with a pitch diameter between 125 and 280 mm (planets studied in the first analysis), the tooth thickness tolerance is 30 μm .

2.4. Statistical methodologies

In order to include the uncertainty associated with the manufacturing processes of planets, a study of the applications has been carried out, in which methodologies that include uncertainties of any type have been used in deterministic numerical models. Among

Table 2

Tolerance value according to DIN-3967 [20], depending on the pitch diameter and gear quality.

Reference diameter (mm)		Tolerance series (μm)				
over	up to	21	22	23	24	25
–	10	3	5	8	12	20
10	50	5	8	12	20	30
50	125	6	10	16	25	40
125	280	8	12	20	30	50
280	560	10	16	25	40	60

the different statistical methods analysed, two of them have been differentiated and studied in depth -MMC and Taguchi's method-, as they are potentially the most appropriate to incorporate into the application under study. The MMC can be defined as a series of mathematical/statistical methods used to obtain a probabilistic solution to a stochastic process and is the most widespread and oldest of those analysed. To do this, the generation of random numbers is utilised, which are used as values of the input variables in the problem, and defining, based on these variables, the probability function of the solution or outputs of the problem.

On the other hand, Taguchi's method is exposed as an efficient tool for the design and optimisation of processes and products, because it focuses on the identification and evaluation of the variables with the greatest influence on the process, on the reduction of the effects of uncontrollable factors, and on the reduction of the variation of the performance of the process [53]. Other authors identify Taguchi's Method as a technique that helps to obtain an optimal combination of design parameters so that the product is functional and with a high level of quality [54]. Moreover, as a complementary technique, the method of orthogonal arrays is generally used, which are partial factorials for carrying out the experiment. In other words, Taguchi's method proposes to analyse the process in its "Full factorial", which evaluates all the possible combinations of parameters and their levels, however, there are techniques such as the one mentioned, which allow the number of simulations to be further reduced. This will be interesting in cases where the simulations are very computational and timely demanding and, therefore, it is not possible to analyse the entire spectrum of possible combinations, simulating just a part of this spectrum which is significant.

One representative example of both methods under study is [44], where the variability of the spur gear transmission critical speed induced by misalignment and manufacturing errors in the teeth was evaluated. With MMC, 20,000 simulations were assessed, in which the distribution of misalignment and profile errors follow a Gaussian probability function, comparing the results with Taguchi's method ones. The results show a small dispersion between methods for two load cases, both in terms of peak-to-peak error of the static transmission error, as well as stresses and stiffness. To be more precise, the difference between MMC and Taguchi's for the mean value of peak-to-peak transmission error and stiffness was 8% and 0.4%, for the high-load case, and 0.3% and 0.2%, for the low-load case.

Taking into account the state of knowledge [36,39,40,44,45] and based on the experience with the gear transmission manufacturer, in order to define the behaviour of the tooth thickness error in the manufacturing process, a normal or Gaussian distribution function is chosen.

In addition, considering the maximum tolerance (e.g. 30 μm in the first analysis) and the "3 σ rule"¹ in normal distribution functions, in order to develop the MMC and emulate the manufacturing process of the planets, it has been included a Gaussian function with null mean and standard deviation of 5 μm (Fig. 5(a)). For Taguchi's method, five thickness error levels have been chosen ($-\sqrt{2}\sigma$, $-\frac{\sqrt{2}}{2}\sigma$, 0, $\frac{\sqrt{2}}{2}\sigma$ and $\sqrt{2}\sigma$), in order to obtain the same standard deviation of 5 μm , and therefore the results are comparable (Fig. 5(b)).

3. Case of study and test set-up

The main characteristics of the two gear transmission configurations are shown in Table 3. These geometrical characteristics have been scaled accordingly from a transmission used in the first stage of a 2.5-MW wind turbine, which cannot be disclosed for confidentiality reasons. This scale factor follows the trend set by the DIN-3967 [20], which states the variability of the tolerance with the gear size. Furthermore, these geometrical characteristics have been chosen and calculated so that they comply with their configuration (ESIP and ESSP) and that, in turn, their results are comparable. Profile shift factor and tip relief value are null for the evaluated planetary gears.

On the other hand, the stiffness of the elements that support the sun is taken into account, which implies that its centre of rotation can vary its position. In the case of application, this total stiffness has been modelled as lumped parameter with a value of 10⁷N/m in both directions, considering the previous geometry and following [16,55].

With respect to the test set-up, in this study, two analyses have been performed; first, an evaluation of MMC and Taguchi's methods and second, a sensitivity assessment of the error tolerance. The former aim is to shed some light on which methodology should be used in this specific application to determine the output distribution function. Whilst, the latter is focused on determining the statistical influence of the tooth thickness tolerance on the transmission performance, represented by the mesh load factor.

¹ 3 σ rule establishes that, in a gaussian distribution, the 99.7% of the cases are into the interval between -3σ and 3σ , being σ the standard deviation of the sample.

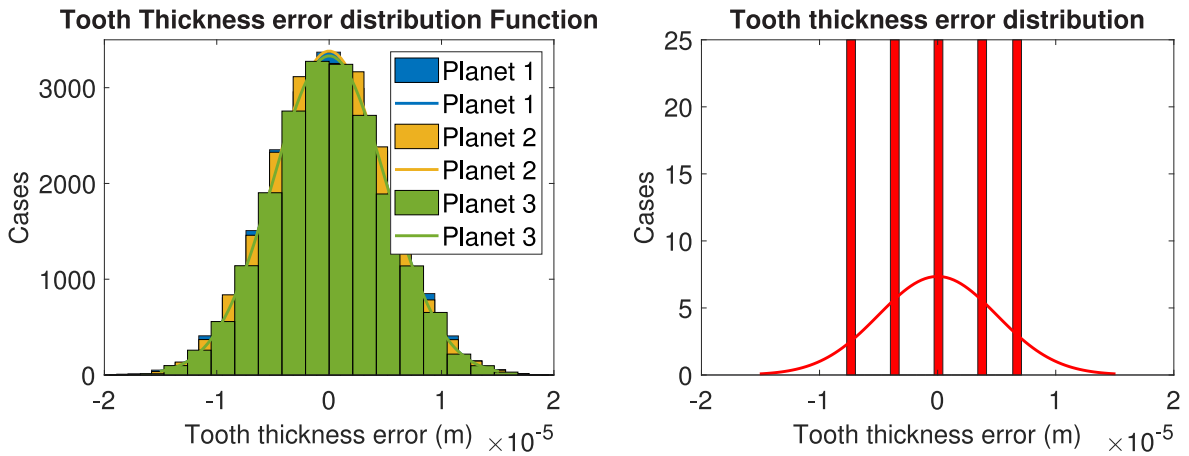


Fig. 5. Gaussian tooth error distribution considered for MMC and Taguchi’s methods when the maximum tolerance is 30 μm.

Table 3
Main parameters of the planetary transmissions elements.

Planetary transmission		
Configuration	ESIP	ESSP
Modulus (<i>m</i>)	4.5 mm	
Pressure angle	20°	
Addendum	<i>m</i>	
Dedendum	1.25 <i>m</i>	
Tip radius	0.05 <i>m</i>	
Ring		
Tooth number	165	166
Pitch diameter(mm)	742.7	747
Planets		
Tooth number	44	45
Pitch diameter(mm)	198	202.5
Sun		
Tooth number	75	74
Pitch diameter(mm)	337.5	333

In the first analysis, the calculation of K_v parameter has been carried out, using MMC and Taguchi’s Method, for two configurations, an ESIP (equally spaced planets in phase) and an ESSP (equally spaced planets in sequential phase). Specifically, a comparison between MMC and Taguchi’s results is presented when the tooth thickness error tolerance is 30 μm (“cd24” quality in DIN-3967 [20]). For MMC, 20,000 random thickness error cases have been generated (Fig. 5(a)) and incorporated into the model previously developed by the authors. This number of simulations was chosen by analysing some stop criteria shown in the Appendix. For the results to be comparable, the same 20,000 cases have been implemented for both configurations (ESIP and ESSP). In the case of Taguchi’s, all possible thickness error combinations have been generated, corresponding to 5 thickness error levels ($-\sqrt{2}\sigma$, $-\frac{\sqrt{2}}{2}\sigma$, 0, $\frac{\sqrt{2}}{2}\sigma$ and $\sqrt{2}\sigma$), resulting in the evaluation of 125 cases (5^3 , where 5 are the chosen levels and 3 the number of planets), as shown in Fig. 5(b).

In the second analysis, a K_v parameter sensitivity assessment has been performed for several tooth thickness error tolerance values (Fig. 6). The limits of tolerance values are 20 and 50 μm, which correspond to the next higher and lower quality in the DIN-3967 [20], “cd23” and “cd25”, respectively (Table 2). In this study, 20,000 cases per tolerance value have been included to obtain each probability function, using MMC, which result into more than 150,000 simulations performed.

4. Results and discussion

4.1. MMC and Taguchi’s method evaluation

In this section, first the results obtained using MMC for both ESIP and ESSP configurations are presented, secondly the ones corresponding to Taguchi’s method and lastly a comparison between them.

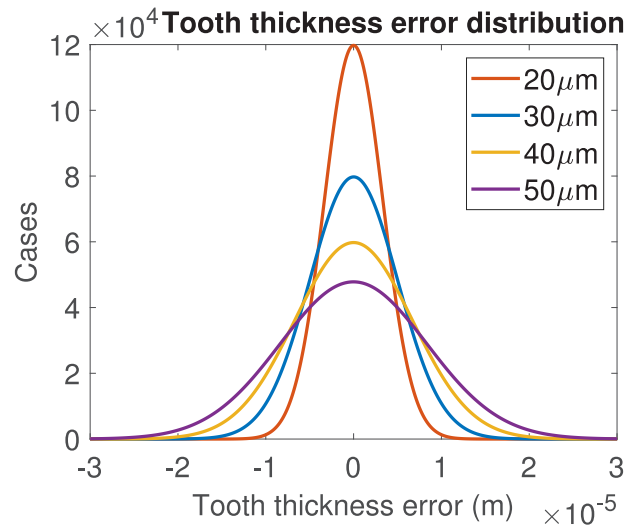


Fig. 6. Gaussian tooth error distribution considered for several maximum tolerances (20:10:50 μm).

4.1.1. Results with MMC

Applying MMC, K_γ parameter has been calculated and represented by means of an histogram, for the ESIP configuration of 3 planets with a floating sun, in Figs. 7(a), 7(b) and, for ESSP configuration, in Figs. 7(c), 7(d).

Both its distribution and cumulative functions have been calculated and analysed for both configurations (Fig. 8), obtaining that, for ESIP, the most probable value of K_γ (mode) is approximately 1.029 and that 1.5% of the specimens will not meet the threshold established in the regulations ($K_\gamma < 1.1$ [19]) for 3-planet wind turbine transmissions. These values corresponding to ESSP configuration are 1.033 and 1.8% respectively.

As additional statistical indicators of the results of K_γ by MMC, for ESIP, its mean and standard deviation are 1.0404 and 0.0226. Moreover, from its distribution function, it can be inferred that K_γ parameter in 1 out of 100 transmissions will be above 1.1056 and in 1 out of 1000 transmissions, it will be above 1.1303. For ESSP case, its mean and standard deviation are 1.0438 and 0.0222, as well as 1 out of 100 transmissions will have a K_γ value above 1.1076 and 1 out of 1000 will be above 1.1318.

4.1.2. Results with Taguchi's method

The K_γ parameter has been also calculated applying Taguchi's Method and represented by means of an histogram in Figs. 9(a), 9(b) for ESIP and in Figs. 9(c), 9(d) for ESSP configurations.

Both its distribution function and its cumulative function have been presented in Fig. 10, obtaining that, for ESIP configuration, the most probable value of K_γ (mode) is approximately 1.037 and that 0.1% of the specimens will not fulfil with the threshold established in the regulations ($K_\gamma < 1.1$ [19]) for 3-planet wind turbine transmissions. In ESSP case, the mode is 1.040 and that 0.2% of the specimens will not fulfil with the threshold.

As additional statistical indicators of the results of K_γ using Taguchi's method, its mean is 1.0403 and its standard deviation is 0.0212. Furthermore, it is inferred from the distribution function of K_γ that 1 out of 100 transmissions will have a value above 1.0918 and 1 out of 1000 transmissions will have a K_γ value above 1.1013. For ESSP configuration, its mean and standard deviation are 1.0437 and 0.0207 respectively, as well as 1 out of 100 transmissions will have a value above 1.0942 and 1 K_γ out of 1000 will be above 1.1034.

4.1.3. Synthesis and comparative of the results

In summary, the distribution function obtained for the configurations and methods analysed (Fig. 11), as well as the most representative values of the parameter K_γ (Table 4), are presented. It can be observed that blue colour is reserved for MMC and red for Taguchi's method, as well as, solid lines correspond to ESIP configuration and dashed to the ESSP.

From the results, it is deduced that the configuration in sequential phase produces higher values of K_γ parameter. This fact implies that the most charged path (most charged planet) has a higher value in ESSP configuration than in the ESIP. In the comparison between methods, it is observed that MMC consumes more computational resources, requiring 20,000 simulations, than Taguchi's Method which requires 125 cases. On the other hand, it can be deduced that MMC produces more reliable results in terms of the distribution function of K_γ parameter. However, it is noticeable that the mean and standard deviation of both methods are practically the same. Therefore, it can be concluded that if only a reference value of the response is to be obtained, Taguchi's method provides a more computationally efficient approach. However, focusing on the output parameter distribution function, result as reliable as possible is sought. Hence, the MMC approach provides a more appropriate result to this specific application.

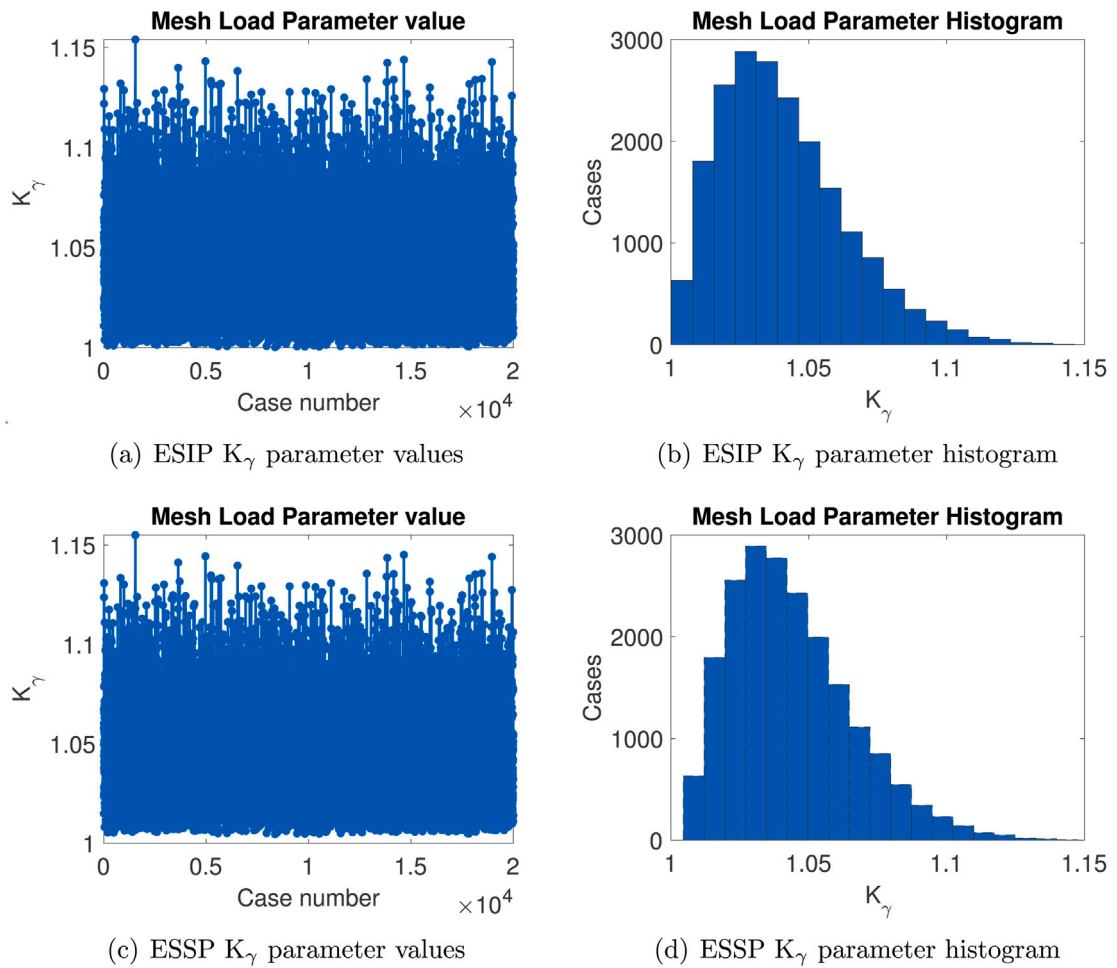


Fig. 7. K_γ values of 20,000 cases of planet tooth thickness error (left) and histogram (right) using MMC method for ESIP (above) and ESSP (below) configurations.

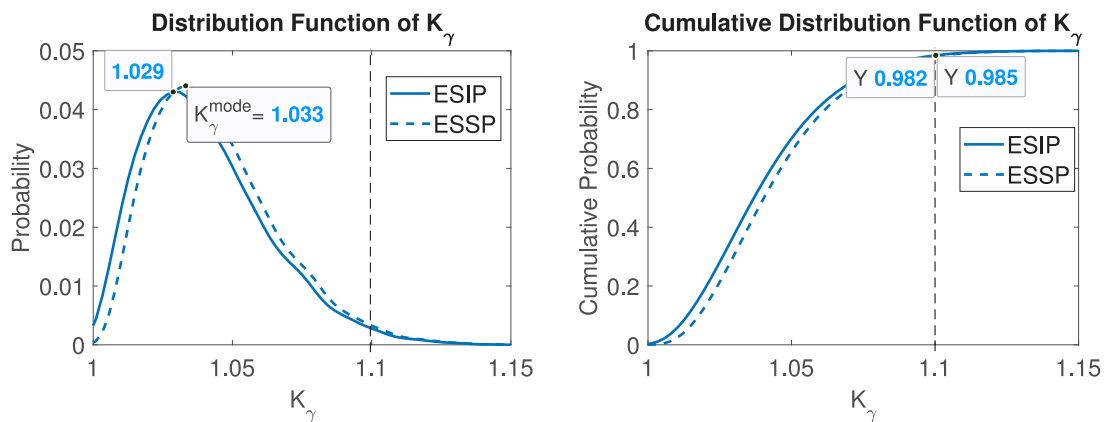


Fig. 8. K_γ distribution function (left) and cumulative distribution function (right) for ESIP configuration.

4.2. Error tolerance sensitivity analysis

In this section, the results obtained using MMC for both ESIP and ESSP configurations are presented when several maximum tolerance values are implemented, in order to evaluate the statistical impact of a better, or worse, quality during the manufacturing

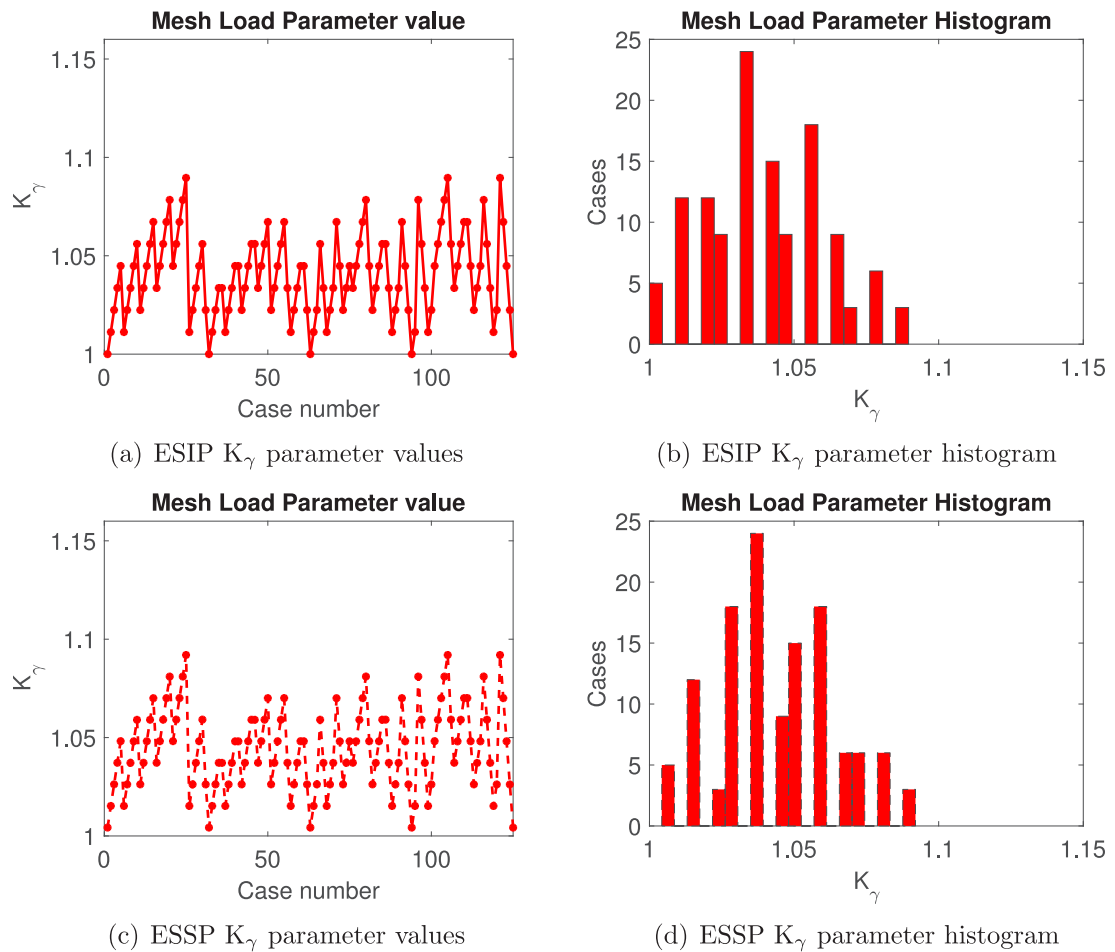


Fig. 9. K_γ values of 125 cases of planet tooth thickness error (left) and histogram (right) using Taguchi's method for ESIP (above) and ESSP (below) configurations.

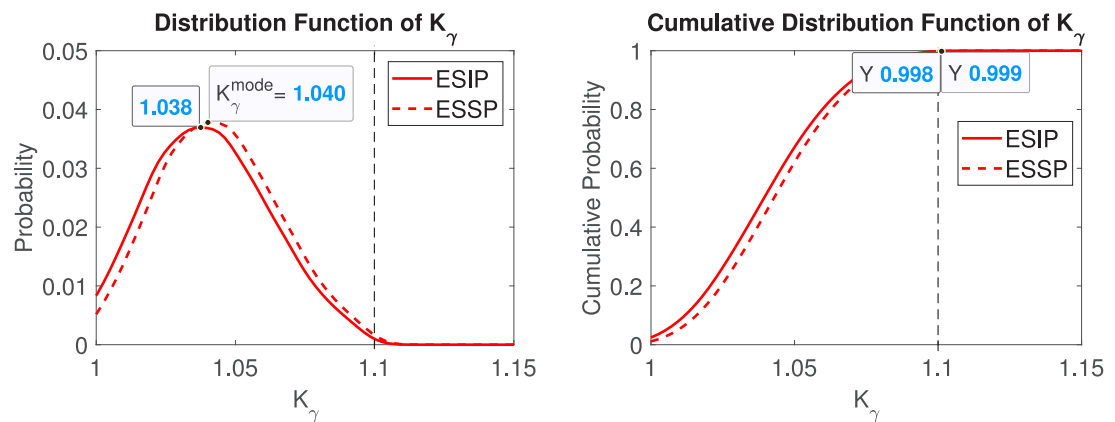


Fig. 10. K_γ distribution function (left) and cumulative distribution function (right) using Taguchi's method.

process on K_γ behaviour. This assessment is intimately connected with the maintenance, failure and manufacturing costs, which in turn could lead to a better balance among them.

The corresponding distribution function for each tolerance value is presented in Fig. 12, in solid line for ESIP configuration and in dash for ESSP, in order to compare between configurations. The implemented tooth thickness error of the 20,000 cases per tolerance value were presented in Section 3 (Fig. 6).

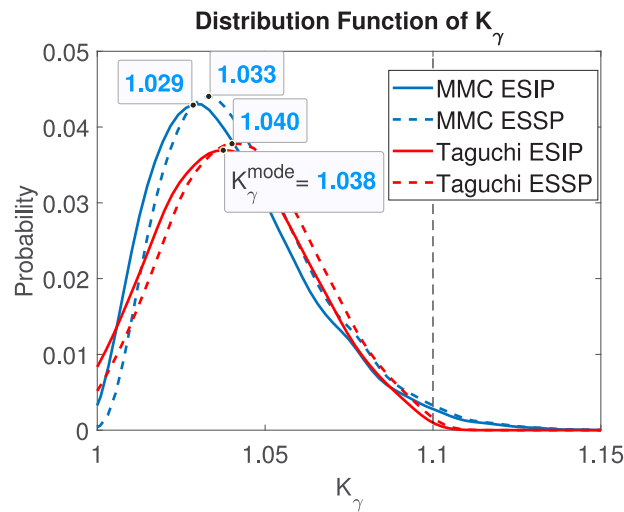


Fig. 11. K_γ parameter value for ESIP and ESSP using MMC y Taguchi's methods.

Table 4
Representative K_γ values for ESIP and ESSP.

		Mode	$P(K_\gamma > 1.1)$	Mean	Std.Dev.	$K_\gamma (P > 0.99)$	$K_\gamma (P > 0.999)$
MMC	ESIP	1.029	1.5%	1.040	0.023	1.106	1.130
	ESSP	1.033	1.8%	1.044	0.022	1.108	1.132
Taguchi	ESIP	1.038	0.1%	1.040	0.021	1.092	1.101
	ESSP	1.040	0.2%	1.044	0.021	1.094	1.103

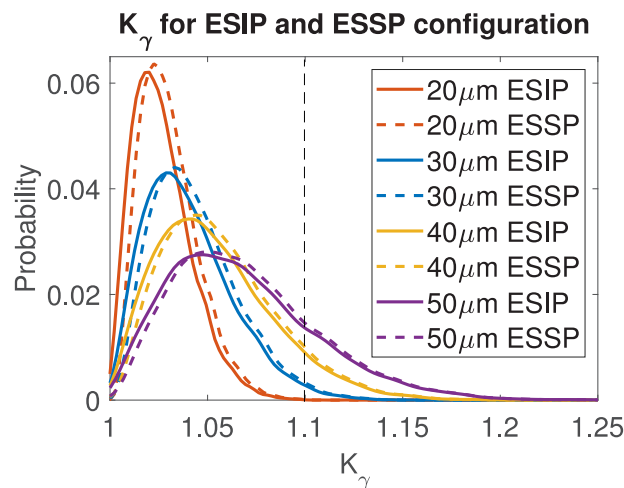


Fig. 12. Comparison between K_γ distribution function for ESIP and ESSP configurations.

From the results, for ESSP configuration, the K_γ mode is higher than for ESIP one and with higher probability. Nevertheless, the configuration does not affect notably to the number of transmissions which are not fulfilling with the K_γ limit of 1.1 imposed by IEC-61400 standard [19]. This means that the ESSP transmission most charged path is subjected to a higher load than the one corresponding to ESIP, however, it should not be a factor to discard them for the application, since they have advantages from a dynamic point of view, mainly attenuating or even making disappear some vibration modes [56].

Lastly, for visualisation and maximum tolerance assessment purposes, the same information is gathered in Fig. 13, discerning between ESIP and ESSP results and marking the mode of each distribution function.

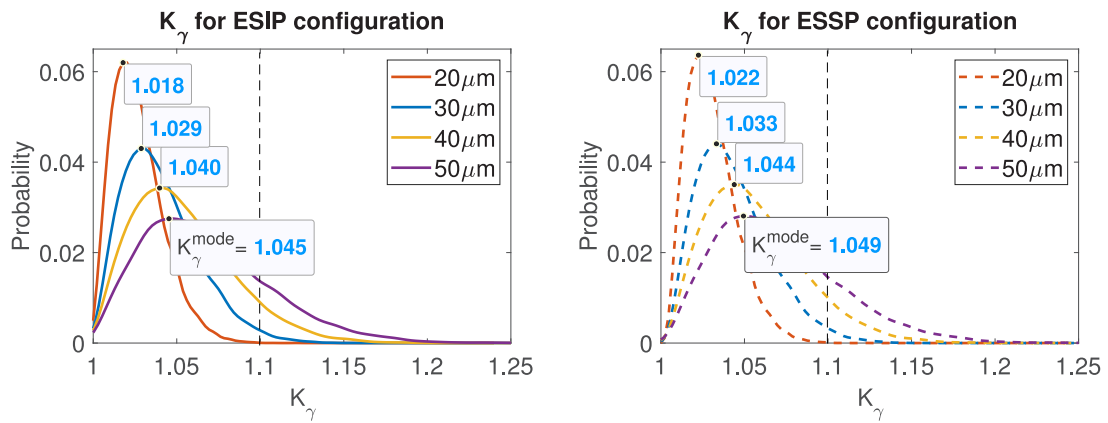


Fig. 13. K_γ distribution function for ESIP (left) and ESSP (right) configurations when several tolerance values are implemented.

Table 5
Representative K_γ values for ESIP and ESSP.

	20 μm		30 μm		40 μm		50 μm	
	ESIP	ESSP	ESIP	ESSP	ESIP	ESSP	ESIP	ESSP
Mode	1.018	1.022	1.029	1.033	1.040	1.044	1.045	1.049
$P(K_\gamma > 1.1)$	0.01%	0.02%	1.55%	1.84%	8.09%	8.93%	18.6%	19.9%
Mean	1.027	1.030	1.040	1.044	1.054	1.057	1.067	1.070
Std. Dev.	0.015	0.015	0.023	0.022	0.030	0.030	0.038	0.037
$K_\gamma (P > 0.99)$	1.071	1.074	1.106	1.108	1.141	1.142	1.176	1.177
$K_\gamma (P > 0.999)$	1.090	1.092	1.130	1.132	1.178	1.178	1.223	1.223

From the results, it can be observed that the higher the tolerance is, the higher the number of transmissions which do not fulfil with K_γ limit of 1.1, as expected. Moreover, the K_γ mode is higher with the tolerance increment, however, this mode has a lower probability, observing that the probability function is flattening with the tolerance increment.

Moreover, the most representative parameters of the density function are gathered in Table 5, for the reader to be able to compared among them.

5. Conclusions

In this work, a probability analysis of K_γ parameter in wind-turbine planetary transmissions with ESIP and ESSP configurations has been carried out, when the planets have thickness errors inherent to their manufacturing process. For this, two statistical methods have been used, Method of Monte Carlo (MMC) and Taguchi’s Method, from which thickness errors have been generated following a Gaussian statistical distribution function. These errors have been incorporated into the model previously developed by the authors, obtaining the K_γ parameter of the studied planetary transmissions, for several tolerance values obtained from DIN-3967.

Regarding the comparison between statistical methods, it is concluded that MMC consumes more computational resources than Taguchi’s Method, although it provides more reliable results in terms of the distribution function of K_γ parameter. Therefore, for this application, MMC is more suitable, since the K_γ probabilistic function was sought. Nevertheless, it is not negligible that the mean and standard deviation provided by both methods are practically the same. Thus, if only a reference K_γ value is to be obtained, Taguchi’s method provides sufficiently accurate results and also a more computationally efficient approach.

From the analysis of configurations, it is deduced that the configuration in sequential phase (ESSP) produces higher values of K_γ parameter than in equispaced in phase (ESIP) one in probabilistic terms. This fact implies that the most charged path has a higher value in ESSP configuration than in the ESIP, and therefore, more probabilities of malfunctions in operation. Moreover, ESSP results shows that K_γ mode is higher than ESIP and with higher probability. Nevertheless, the configuration does not affect notably to the number of transmissions which are not fulfilling with the K_γ limit of 1.1 imposed by IEC-61400 standard. From all the above, it can be concluded that, although it was expected that ESSP generates higher K_γ values than ESIP, this aspect should not be a factor to discard them for the application, since the load sharing behaviour is not critically worsened and the dynamics advantages could compensate it.

From the tolerance value assessment, the higher the tolerance is, the higher the number of transmissions which do not fulfil with the K_γ limit of 1.1. Furthermore, the K_γ mode is higher with the tolerance increment, as well as this mode has lower probability, observing that the probability function is flattening with this tolerance increment.

As future work, it is envisaged to stochastically study the effect of the pinhole position errors added to the tooth thickness one, in order to analyse the combination of mounting and manufacturing error effects.

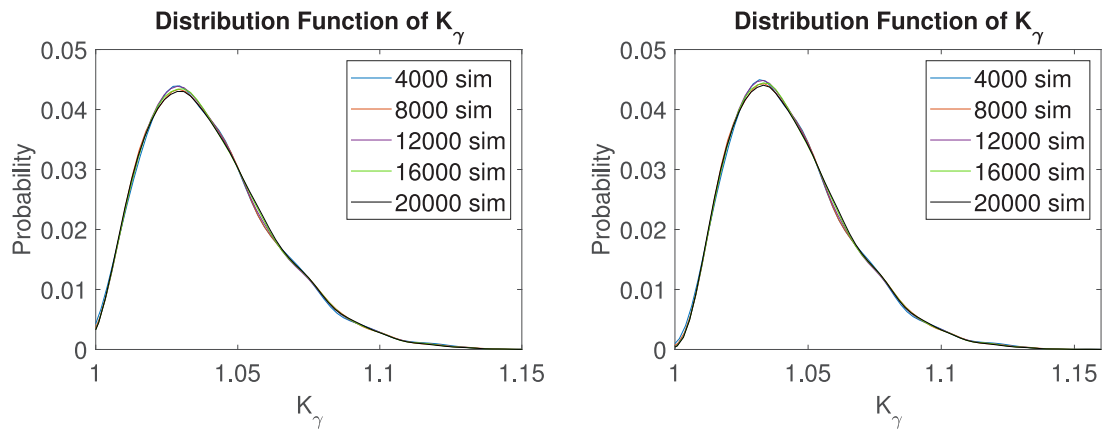


Fig. A.14. Evolution of the distribution function of the value K_γ for the ESIP (left) and ESSP (right) configuration, when the tooth thickness error tolerance is $30\ \mu\text{m}$.

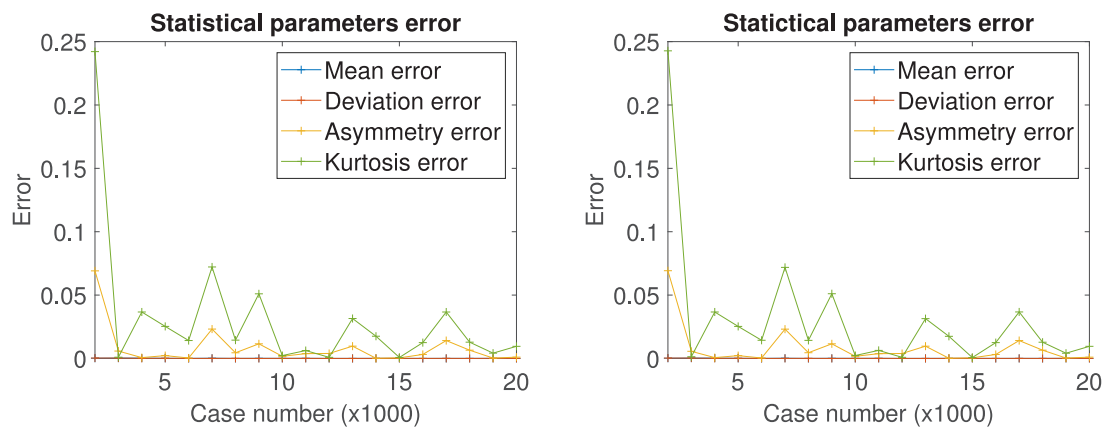


Fig. A.15. Evolution of the statistical parameters of the distribution function of K_γ for the configuration ESIP (left) and ESSP (right).

Declaration of competing interest

The authors declare that they have no known competing financial interests or personal relationships that could have appeared to influence the work reported in this paper.

Data availability

The data has been disclosed in the manuscript, however the code will not be disclosed.

Acknowledgements

This work has been supported by project PID2020-116213RB-I00 and PID2020-116572RA-I00 funded by the Spanish Ministry of Science and Innovation, as well as SIEMENS GAMESA RENEWABLE ENERGY S.A.

Appendix. Stop criteria

As an additional study, various stopping criteria have been analysed to perform MMC and it was concluded that, for this case study, 20,000 simulations are sufficient (even 15,000 simulations would have been sufficient). Next, for the two configurations analysed, the evolution of the distribution function of K_γ parameter is presented, with a linear progression of 4000 simulations (Fig. A.14), when the tooth thickness error tolerance is $30\ \mu\text{m}$.

On the other hand, various statistical parameters have been calculated, such as the mean, standard deviation, asymmetry coefficient and Kurtosis coefficient (μ , σ , s and k , respectively), and their variation has been analysed every 1000 simulations, obtaining its error as:

$$\begin{aligned} e_{\mu} &= \mu_{1,000-(n+1)} - \mu_{1,000n} \\ e_{\sigma} &= \sigma_{1,000-(n+1)} - \sigma_{1,000n} \\ e_s &= s_{1,000-(n+1)} - s_{1,000n} \\ e_k &= k_{1,000-(n+1)} - k_{1,000n} \end{aligned} \quad (\text{A.1})$$

The evolution of the errors of these parameters has been presented in Fig. A.15, for the two configurations of planetary transmissions studied.

References

- [1] P. Marques, R. Martins, J. Seabra, Power loss and load distribution models including frictional effects for spur and helical gears, *Mech. Mach. Theory* 96 (2016) 1–25.
- [2] E. Mucchi, G. Dalpiaz, A. Fernandez del Rincon, Elasto-dynamic analysis of a gear pump-part IV: Improvement in the pressure distribution modelling, *Mech. Syst. Signal Process.* 50–51 (2015) 193–213.
- [3] C. Nutakor, A. Kłodowski, J. Sapanen, A. Mikkola, J.I. Pedrero, Planetary gear sets power loss modeling: Application to wind turbines, *Tribol. Int.* 105 (2017) 42–54.
- [4] J.I. Pedrero, D. Martinez-Lopez, J. Calvo-Irisarri, M. Pleguezuelos, M.B. Sanchez, A. Fernandez-Sison, Minimum friction losses in wind turbine gearboxes, *Forschung Ingen./Eng. Res.* 86 (2021) 321–330.
- [5] J.I. Pedrero, M. Pleguezuelos, M.B. Sanchez, Influence of meshing stiffness on load distribution between planets of planetary gear drives, *Mech. Mach. Theory* 170 (2022) 1–13.
- [6] D.C. Talbot, A. Kahraman, A. Singh, An experimental investigation of the efficiency of planetary gear sets, *Trans. ASME, J. Mech. Des.* 134 (2012) 839–855.
- [7] X. Liu, Y. Yang, J. Zhang, Resultant vibration signal model based fault diagnosis of a single stage planetary gear train with an incipient tooth crack on the sun gear, *Renew. Energy* 122 (2018) 65–79.
- [8] A. Mbarek, A. Hammami, A. Fernandez-Del-Rincon, F. Chaari, F. Viadero, M. Haddar, Effect of load and meshing stiffness variation on modal properties of planetary gear, *Appl. Acoust.* 147 (2019) 32–43.
- [9] S. Mo, Y. Zhang, Q. Wu, S. Matsumura, H. Houjoh, Load sharing behavior analysis method of wind turbine gearbox in consideration of multiple-errors, *Renew. Energy* 97 (2016) 481–491.
- [10] F. Viadero, A. Fernandez, M. Iglesias, A. De-Juan, E. Liaño, M.A. Serna, Non-stationary dynamic analysis of a wind turbine power drivetrain: Offshore considerations, *Appl. Acoust.* 77 (2014) 204–211.
- [11] C. Zhu, X. Xu, H. Liu, T. Luo, H. Zhai, Research on dynamical characteristics of wind turbine gearboxes with flexible pins, *Renew. Energy* 68 (2014) 724–732.
- [12] A. Fernandez del Rincon, A. Diez-Ibarbia, M. Iglesias, F. Viadero, Gear rattle dynamics: Lubricant force formulation analysis on stationary conditions, *Mech. Mach. Theory* 142 (2019) 1–21.
- [13] M. Iglesias, A. Fernandez del Rincon, A. de Juan, P. Garcia, A. Diez-Ibarbia, F. Viadero, Planetary transmission load sharing: Manufacturing errors and system configuration study, *Mech. Mach. Theory* 111 (2017) 21–38.
- [14] J. Sanchez-Espiga, A. Fernandez del-Rincon-del Rincon, M. Iglesias, F. Viadero, Influence of errors in planetary transmissions load sharing under different mesh phasing, *Mech. Mach. Theory* 153 (2020) 1–17.
- [15] J. Sanchez-Espiga, A. Fernandez del-Rincon-del Rincon, M. Iglesias, F. Viadero, Planetary gear transmissions load sharing measurement from tooth root strains: Numerical evaluation of mesh phasing influence, *Mech. Mach. Theory* 163 (2021) 1–18.
- [16] A. Singh, Application of a system level model to study the planetary load sharing behavior, *J. Mech. Des.* 127 (2005) 469–476.
- [17] A. Bodas, A. Kahraman, Influence of carrier and gear manufacturing errors on the static load sharing behavior of planetary gear sets, *JSME Int. J. Ser. C* 47 (2004) 908–915.
- [18] ISO 6336-1:2019, Calculation of load capacity of spur and helical gears. Basic principles, introduction and general influence factors, 2006, International Organization for Standardization.
- [19] IEC 61400-4:2012, Design requirements for wind turbine gearboxes, 2012, International Electrotechnical Commission.
- [20] DIN 3967:1978, Tooth allowances, tooth thickness tolerances system of gear fits principles: Backlash, 1978, Deutsches Institut für Normung.
- [21] A.M. Al-Shaalán, Reliability Evaluation of Power Systems, Springer Science & Business Media, 2013.
- [22] R. Billinton, H. Chen, R. Ghajar, Time-series models for reliability evaluation of power systems including wind energy, *Microelectron. Reliab.* 36 (1996) 1253–1261.
- [23] E.C. Gonzalez-L., W. Adarme-Jaimes, J.A. Orjuela-Castro, Stochastic mathematical model for vehicle routing problem in collecting perishable products, *DYNA* 82 (2015) 199–206.
- [24] C.E. Azofeifa, Aplicacion de la Simulacion Monte Carlo en el calculo del riesgo usando excel, *Tecnol. Marcha* 17 (2004) 99–109.
- [25] B. D'Amico, F. Pomponi, Accuracy and reliability: A computational tool to minimise steel mass and carbon emissions at early-stage structural design, *Energy Build.* 168 (2018) 236–250.
- [26] R. Billinton, R. Karki, Application of Monte Carlo simulation to generating system well-being analysis, *IEEE Trans. Power Syst.* 14 (1999) 1172–1177.
- [27] F.E. Montmeat, J. Zemkoski, A.D. Patton, D.J. Cumming, Power system reliability II—Applications and a computer program, *IEEE Trans. Power Appar. Syst.* 84 (1965) 636–643.
- [28] A.D. Patton, A.K. Ayoub, C. Singh, Power system reliability evaluation, *Int. J. Electr. Power Energy Syst.* 1 (1979) 139–150.
- [29] S.F. Abdelsamad, W.G. Morsi, T.S. Sidhu, Impact of wind-based distributed generation on electric energy in distribution systems embedded with electric vehicles, *IEEE Trans. Sustain. Energy* 6 (2015) 79–87.
- [30] R. Karki, Reliability of renewable power systems, *Encycl. Sustain. Technol.* 4 (2017) 217–230.
- [31] A. Alferidi, R. Karki, Development of probabilistic reliability models of photovoltaic system topologies for system adequacy evaluation, *Appl. Sci.* 7 (2017) 1–16.
- [32] X. Liu, X. Zheng, L. Wu, S. Deng, H. Pan, J. Zou, X. Zhang, Y. Luo, Techno-ecological synergies of hydropower plants: Insights from GHG mitigation, *Sci. Total Environ.* 853 (2022) 1–12.
- [33] M. Razi, M.A. Yusuff, K.A. Zakaria, A. Putra, Stream flow analysis for small hydropower system based on run-of-river schemes, *ARPN J. Eng. Appl. Sci.* 13 (2018) 1115–1118.

- [34] Y. Wang, Z. Yang, L. Wang, X. Ma, W. Wu, L. Ye, Y. Zhou, Y. Luo, Forecasting China's energy production and consumption based on a novel structural adaptive Caputo fractional grey prediction model, *Energy* 259 (2022) 1–27.
- [35] J. Wang, S. Yang, Y. Liu, R. Mo, Analysis of load-sharing behavior of the multistage planetary gear train used in wind generators: Effects of random wind load, *Appl. Sci.* 9 (2019) 1–12.
- [36] C. Xun, X. Long, H. Hua, Effects of random tooth profile errors on the dynamic behaviors of planetary gears, *J. Sound Vib.* 415 (2018) 91–110.
- [37] J. Zhang, F. Guo, Statistical modification analysis of helical planetary gears based on response surface method and Monte Carlo simulation, *Chin. J. Mech. Eng. (Engl. Ed.)* 28 (2015) 1194–1203.
- [38] H. Alkhadafe, A. Al-Habaibeh, A. Lotfi, Condition monitoring of helical gears using automated selection of features and sensors, *Meas.: J. Int. Meas. Confed.* 93 (2016) 164–177.
- [39] X. Deng, S. Wang, H. Youssef, L. Qian, Y. Liu, Study on the influence of key design parameters on lubrication characteristics of a novel gear system applying Taguchi method, *Struct. Multidiscip. Optim.* 62 (2020) 2833–2847.
- [40] J.R. D'Errico, N.A. Zaino, Statistical tolerancing using a modification of taguchi's method, *Technometrics* 30 (1988) 397–405.
- [41] T. Koide, D. Matsuura, A. Tamura, T. Yasugi, T. Mori, Gear and bearing failure detection using vibration monitoring and mahalanobis-taguchi system, in: *International Design Engineering Technical Conferences and Computers and Information in Engineering Conference*, American Society of Mechanical Engineers, 2015.
- [42] F. Mayeux, E. Rigaud, J. Perret-Liaudet, Dispersion of critical rotational speeds of gearbox: effect of bearings stiffnesses, in: *ISMA International Conference on Noise and Vibration Engineering*, 2007, arXiv.
- [43] N.M. Mehat, N.S. Zakarria, S. Kamaruddin, Investigating the effects of blending ratio and injection parameters on the tensile properties of glass fiber-filled nylon 66 composite gear, *Appl. Mech. Mater.* 548–549 (2014) 43–47.
- [44] N. Driot, E. Rigaud, J. Perret-Liaudet, Variability of critical rotational speeds of gearbox induced by misalignment and manufacturing errors, in: *JSME International Conference on Motion and Power Transmissions*, 2007, pp. 63–67, arXiv.
- [45] S. Sundaresan, K. Ishii, D.R. Houser, A procedure using manufacturing variance to design gears with minimum transmission error, *Trans. ASME, J. Mech. Des.* 113 (1991) 318–324.
- [46] A. Diez-Ibarbia, A. Fernandez del Rincon, P. Garcia, A. de Juan, M. Iglesias, F. Viadero, Assessment of load dependent friction coefficients and their influence on spur gears efficiency, *Meccanica* 53 (2018) 425–445.
- [47] A. Diez-Ibarbia, A. Fernandez-del Rincon, P. Garcia, F. Viadero, Gear rattle dynamics under non-stationary conditions: The lubricant role, *Mech. Mach. Theory* 151 (2020) 1–31.
- [48] A. Fernandez-Del-Rincon, A. Diez-Ibarbia, S. Theodossiades, Gear transmission rattle: Assessment of meshing forces under hydrodynamic lubrication, *Appl. Acoust.* 144 (2019) 85–95.
- [49] M. Iglesias, A. Fernandez del Rincon, A. de Juan, A. Diez-Ibarbia, P. Garcia, F. Viadero, Planetary gear profile modification design based on load sharing modelling, *Chin. J. Mech. Eng. (Engl. Ed.)* 28 (2015) 810–820.
- [50] C. Weber, *The Deformation of Loaded Gears and the Effect on Their Load Carrying Capacity*, Department of Scientific and Industrial Research, London, 1951.
- [51] J. Brauer, A general finite element model of involute gears, *Finite Elem. Anal. Des.* 40 (2004) 1857–1872.
- [52] E. Wildhaber, Measuring tooth thickness of involute gears, *Amer. Mach.* 59 (1923) 551.
- [53] G. Box, Signal-to-noise ratios, performance criteria, and transformations, *Technometrics* 30 (1988) 1–17.
- [54] R.S. Rao, C.G. Kumar, R.S. Prakasham, P.J. Hobbs, The Taguchi methodology as a statistical tool for biotechnological applications: A critical appraisal, *Biotechnol. J.* 3 (2008) 510–523.
- [55] C. Zhang, J. Wei, F. Wang, S. Hou, A. Zhang, T.C. Lim, Dynamic model and load sharing performance of planetary gear system with journal bearing, *Mech. Mach. Theory* 151 (2020) 1–22.
- [56] V.K. Ambarisha, R.G. Parker, Suppression of planet mode response in planetary gear dynamics through mesh phasing, *J. Vib. Acoust.* 128 (2006) 133–142.